Distinct Populations of HCN Pacemaker Channels Produce Voltage-dependent and Voltage-independent Currents

Catherine Proenza and Gary Yellen

Department of Neurobiology, Harvard Medical School, Boston, MA 02115

Hyperpolarization-activated HCN pacemaker channels are critical for the generation of spontaneous activity and the regulation of excitability in the heart and in many types of neurons. These channels produce both a voltage-dependent current (I_h) and a voltage-independent current (I_{inst} or VIC). In this study, we explored the molecular basis of the voltage-independent current. We found that for the spHCN isoform, VIC averaged ∼4% of the maximum HCN conductance that could be activated by hyperpolarization. Cyclic AMP increased the voltage-independent current in spHCN to ∼8% of maximum. In HCN2, VIC was ∼2% of the maximal current, and was little affected by cAMP. VIC in both spHCN and HCN2 was blocked rapidly both by ZD7288 (an HCN channel blocker that is thought to bind in the conduction pore) and by application of Cd^{2+} to channels containing an introduced cysteine in the pore (spHCN-464C or HCN2-436C). These results suggest that VIC flows through the main conduction pathway, down the central axis of the protein. We suspected that VIC simply represented a nonzero limiting open probability for HCN channels at positive voltages. Surprisingly, we found instead that the spHCN channels carrying VIC were not in rapid equilibrium with the channels carrying the voltage-dependent current, because they could be blocked independently; a single application of blocker at a depolarized potential essentially eliminated VIC with little change in I_h. Thus, VIC appears to be produced by a distinct population of HCN channels. This voltage-independent current could contribute significantly to the role of HCN channels in neurons and myocytes; VIC flowing through the channels at physiological potentials would tend to promote excitability by accelerating both depolarization and repolarization.

INTRODUCTION

Hyperpolarization-activated, cyclic nucleotide sensitive (HCN or "pacemaker") ion channels are highly expressed in the mammalian heart and central nervous system, where they produce slowly activating currents known as I_h, I_f, or I_q (Brown et al., 1979; Brown and DiFrancesco, 1980; Halliwell and Adams, 1982; Pape and McCormick, 1989). These channels are permeable to both sodium and potassium, resulting in a reversal potential of ∼−20 mV in physiological solutions.

Four mammalian HCN isoforms (HCN1–4) and a related channel from sea urchin (spHCN) have been cloned and expressed in heterologous systems, where they produce hyperpolarization-activated currents that resemble the native currents (Santoro et al., 1997; Gauss et al., 1998; Ludwig et al., 1998; Santoro et al., 1998; Ishii et al., 1999). In addition to their activation by hyperpolarization, HCN channels are also modulated by direct binding of cAMP to a consensus cyclic nucleotide binding domain in the COOH terminus. In the mammalian channels, binding of cAMP shifts the voltage dependence of activation to more positive potentials, whereas in spHCN, cAMP relieves a rapid inactivation
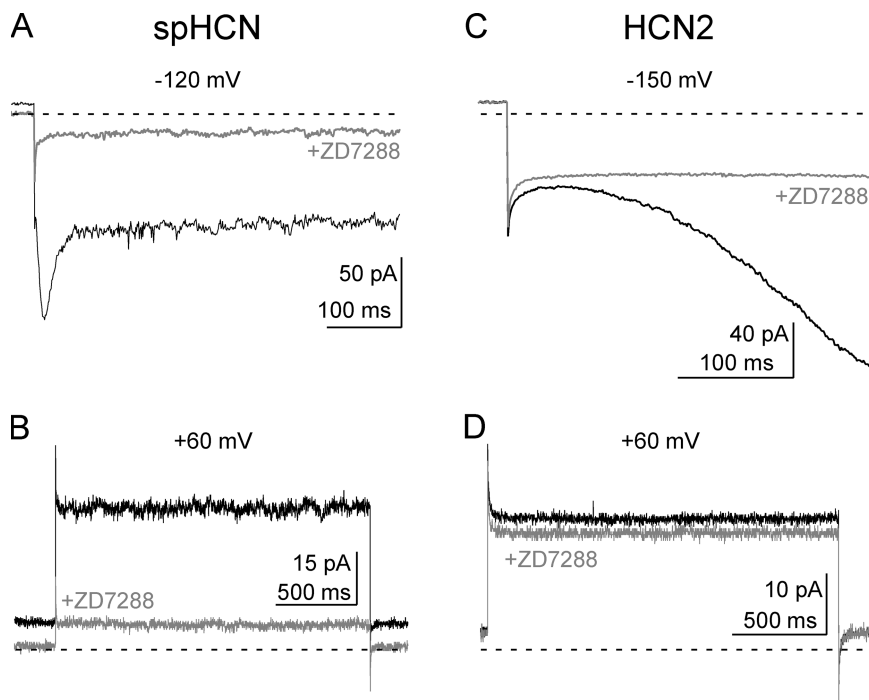
process. This inactivation appears to occur not by closure of a specialized inactivation gate, but by reclosure of the main intracellular activation gate of the channels (Shin et al., 2004), which, like that of depolarization-activated K^+ channels, is composed of the intracellular part of the S6 transmembrane domain (Shin et al., 2001; Rothberg et al., 2002; Rothberg et al., 2003). Closure of the activation gate limits access of ions and the blocker ZD7288 to the pore of HCN channels from the intracellular side of the membrane (Shin et al., 2001; Rothberg et al., 2002).

In addition to I_h, a voltage-independent current (I_{inst} or VIC) accompanies expression of HCN2 and HCN1 channels (Proenza et al., 2002; Macri and Accili, 2004). This current is thought to be produced by HCN channels because it depends on surface expression of the channels, because it has a reversal potential similar to that of I_h, and because its amplitude is correlated with that of I_h. The voltage-independent current could play a very important role in determining the excitability of cells where HCN channels are expressed, yet many mechanistic questions remain about how these voltage-dependent channels could also produce a voltage-independent current.

Correspondence to Gary Yellen: gary_yellen@hms.harvard.edu

C. Proenza's present address is University of Connecticut, Department of Physiology and Neurobiology, 75 N. Eagleville Rd, U-4156 Storrs, CT 06269.

Abbreviations used in this paper: HCN, hyperpolarization-activated, cyclic nucleotide sensitive; VIC, voltage-independent current.

A   spHCN

-120 mV

+ZD7288

50 pA
100 ms

B   +60 mV

15 pA
500 ms

+ZD7288

C   HCN2

-150 mV

+ZD7288

40 pA
100 ms

D   +60 mV

+ZD7288

10 pA
500 ms

Figure 1. Voltage-independent currents produced by spHCN and HCN2 pacemaker channels. Currents elicited by voltage steps to -120 mV (A) and $+60$ mV (B) for spHCN, or to -150 mV (C) and $+60$ mV (D) for HCN2. Currents were recorded in the absence (black traces) or presence (gray traces) of 100 μM ZD7288, an HCN channel blocker. The holding potential for all recordings was $+10$ mV and the zero current level is marked by the dotted lines. The VIC is defined as the ZD7288-sensitive current seen immediately upon stepping the voltage to hyperpolarized potentials, or as the ZD7288-sensitive steady-state current at $+60$ mV.

We used the ability of the intracellular activation gate to limit access of blockers to the pore of HCN channels to explore the molecular basis of the voltage-independent current. We found that VIC was blocked by state-dependent HCN blockers, suggesting that it flows through the main conduction pathway of HCN channels that have activation gates in an open position. Surprisingly, VIC could be blocked independently of I_h, suggesting that it is produced by a separate population of channels that is not in rapid equilibrium with the main population of voltage-dependent channels.

MATERIALS AND METHODS

Expression of Recombinant HCN Channels

HCN channels were transiently expressed in human embryonic kidney 293 cells (HEK293; American Type Culture Collection) using electroporation as described previously (Shin et al., 2001). Channels were cotransfected with the πH3-CD8 plasmid (Seed and Aruffo, 1987), which expresses the α subunit of the human CD8 lymphocyte antigen. Cells expressing the CD8 antigen were identified by decoration with antibody-coated beads (Jurman et al., 1994).

As in our previous experiments, spHCN channels contained the M349I mutation to increase functional expression levels (Shin et al., 2001). The spHCN-464C mutant channel has been previously described (Rothberg et al., 2002). The HCN2-436C mutant channel was constructed using overlapping PCR mutagenesis and the mutation was confirmed by automated DNA sequencing (Biopolymers Facility, Harvard Medical School).

Solutions and Electrophysiological Recordings

All experiments were performed at room temperature on excised inside-out patches (Hamill et al., 1981) from identified transfected cells 1–2 d after transfection. Currents were digitized at

5–10 kHz and low-pass filtered at 1–2 kHz. The holding potential for all experiments was $+10$ mV.

The standard intracellular solution consisted of (in mM) 160 KCl, 1 $MgCl_2$, 10 HEPES, 1 EGTA, pH 7.4 with KOH. The extracellular solution was the same, but without EGTA. In some experiments, 100 μM cAMP (Sigma-Aldrich), or 100 μM ZD7288 (Tocris) were included in the intracellular solution as noted. For experiments using Cd^{2+}, the control intracellular solution contained 20 μM EGTA. This solution was rapidly changed to a solution containing 20 μM Cd^{2+} and lacking EGTA.

Voltage-dependent I_h amplitudes were reported as the difference in time-dependent current between the beginning and end of a hyperpolarizing voltage step. VIC was reported as the average steady-state current at $+60$ mV. Nonspecific leakage currents, defined as those remaining after complete block by ZD7288 (or Cd^{2+}, in spHCN-464C) were subtracted to give the net VIC. Data are reported as mean $\pm$ SEM.

RESULTS

ZD7288-sensitive, Time- and Voltage-independent Conductance Produced by spHCN and HCN2

The HCN channel blocker ZD7288 acts from the intracellular side of the membrane. It is thought to bind in the pore of the channels because it can be trapped behind the closed activation gate, and because mutations in the pore vestibule alter the reversibility of its binding to either spHCN or HCN1 channels (Shin et al., 2001). Fig. 1 shows that, in addition to blocking I_h, ZD7288 also blocked a VIC in excised inside-out patches from HEK293 cells expressing either the HCN2 or spHCN pacemaker channel isoform. This current was evident either as the instantaneous inward current at hyperpolarized potentials (after the capacitive transient but
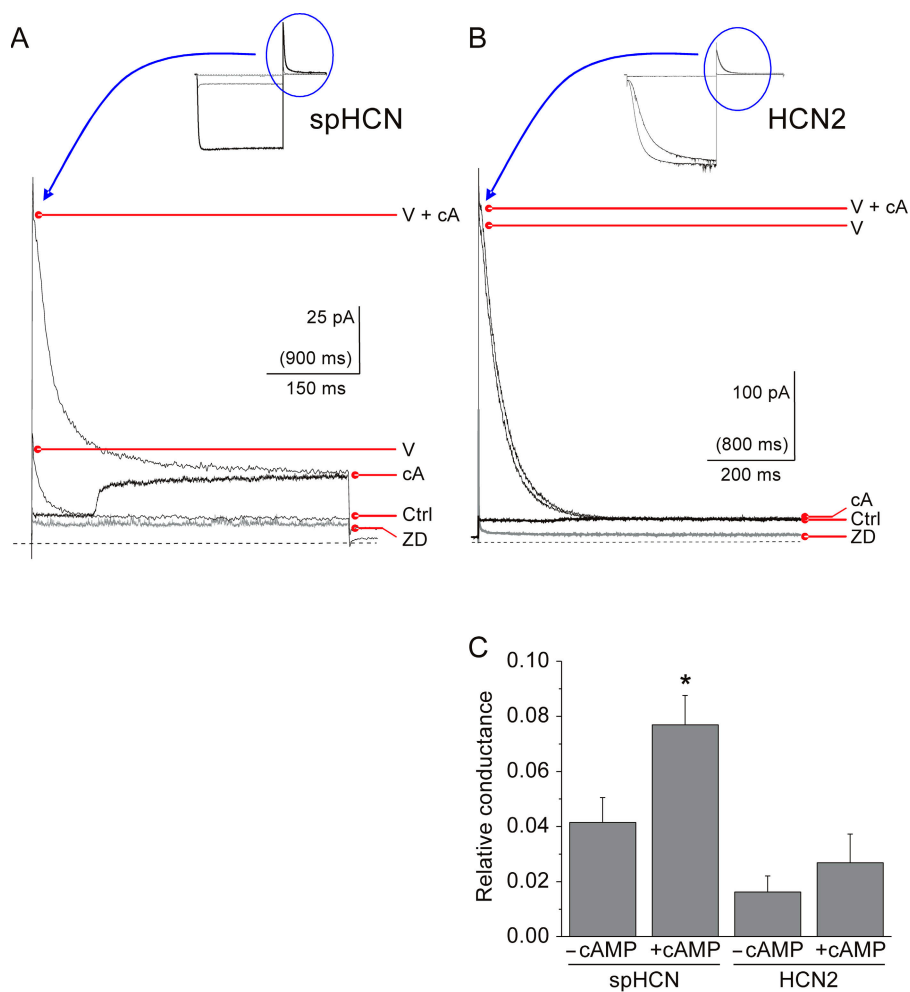
Figure 2. Relative amplitude of the VIC and its response to cAMP. Maximal outward currents through spHCN channels (A) or HCN2 channels (B) at +60 mV were measured as tail currents in the presence of 100 μM cAMP (thin lines) after maximally activating voltage steps (to −120 mV for spHCN and −150 mV for HCN2). The full current traces are shown in the insets (also shown for comparison are currents in the absence of cAMP). The peak tail currents elicited by voltage and cAMP are marked V+cA, and those in the absence of cAMP are marked V. Overlaid on the tail currents are VIC currents elicited by voltage steps directly from +10 to +60 mV (thick black lines). These voltage steps to +60 mV were conducted on a slower time scale, as indicated by the units in parentheses on the horizontal scale bars. This allowed rapid application of 100 μM cAMP to the intracellular face of the patches during the voltage steps. In spHCN, cAMP elicited a fairly rapid increase in VIC. In HCN2, application of cAMP produced little change in VIC. VIC current amplitudes in the presence or absence of 100 μM cAMP are indicated as cA or Ctrl. Endogenous currents and nonspecific leak can be seen as the current remaining in the presence of 100 μM ZD7288 (marked ZD, thick gray lines). The zero current level is indicated by the dashed lines. (C) The average relative conductance of VIC is plotted for spHCN ($n = 8$) and HCN2($n = 5$) in the presence or absence of 100 μM cAMP. Relative conductance of VIC was calculated by subtracting the ZD7288 baseline and normalizing to the amplitude of the peak tail current in the presence of cAMP (baseline ZD7288 was also subtracted from the tail currents). The asterisk denotes a significant effect of cAMP on spHCN (paired t test, P < 0.005). The difference between control and cAMP was not significant for HCN2 (paired t test, P = 0.14).

before the voltage-dependent current begins to activate; Fig. 1, A and C), or as the steady-state outward current during a voltage step to +60 mV (Fig. 1, B and D). The outward current was observed at a potential at least 70 mV positive to the foot of the conductance–voltage relation (the foot of the g-V, defined as the voltage at which <5% of the voltage-dependent conductance is activated, is ∼−10 mV for spHCN and ∼−60 mV for HCN2 in our expression system; Shin et al., 2004).

We next determined the relative contribution of VIC to the total HCN current. The maximum total HCN current was measured at +60 mV by exposing the patch to 100 μM cAMP and applying a maximally activating prepulse to a negative voltage (−120 mV for spHCN and −150 mV for HCN2). This maximal current was seen as a transient outward tail current (Fig. 2, A and B); it was measured immediately after the step to +60 mV, and the leak current remaining after ZD7288 application (at the end of the experiment) was subtracted. VIC was measured as the steady-state, ZD7288-sensitive out-ward current at +60 mV, both in the presence and absence of cAMP. In the absence of cAMP, VIC averaged 4.1 ± 0.9% ($n = 8$) of the total HCN current for spHCN and 1.6 ± 0.6% of the total current for HCN2 ($n = 5$).

In spHCN, cAMP significantly increased the voltage-independent current (seen for example as the stepwise increase produced by solenoid application of cAMP during the step to +60 mV; Fig. 2 A). The average cAMP-induced increase in spHCN-VIC was 2.8 ± 0.7–fold (to 7.7 ± 1.1% of the total current; Fig. 2 C; P < 0.005, paired t test). Small increases in HCN2-VIC were sometimes seen with cAMP application, but the average change was not statistically significant.

(This differs from a previous report that cAMP decreased instantaneous current in HCN2 (Proenza et al., 2002). This difference could be a result of the different recording methods: whole cell in the previous report compared with cell-free inside-out patches in the present report. Channel-associated proteins and other cellular factors retained in whole cell recordings may
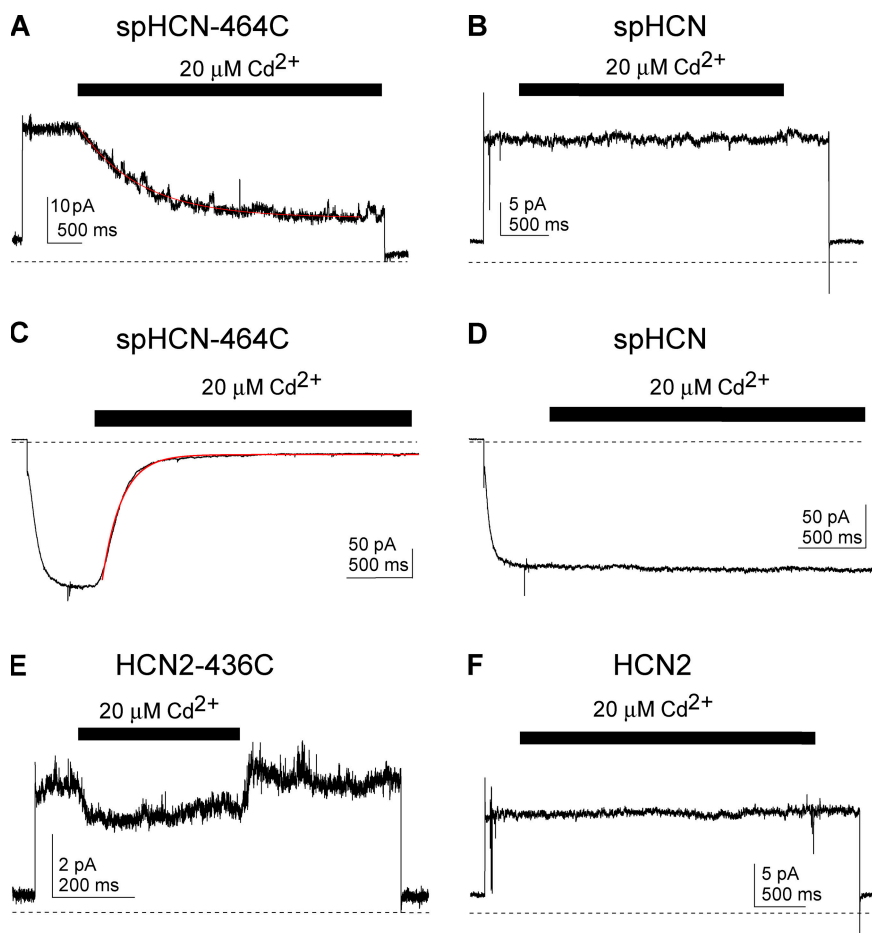
Figure 3. Block of VIC and I_h by Cd^{2+} in spHCN-464C and HCN2-436C. Cadmium ions blocked spHCN-464C currents at +60 mV (A) and −120 mV (C), but not control spHCN currents under the same conditions (B and D). Cadmium ions could also block HCN2-436C currents at +60 mV (E), but not wild-type HCN2 (F). All currents were measured in the constant presence of 100 μM cAMP. 20 μM Cd^{2+} was rapidly applied to the patches via a solenoid perfusion system at the times indicated by the black bars. The red lines in A and C are single exponential fits to the time course of the block, which were used to determine the blocker on-rates. No effect of 20 μM Cd^{2+} was observed for wild-type spHCN or HCN2 channels in response to these acute applications, though we have noticed a block of the time-dependent current with prolonged applications (20 μM Cd^{2+} for >1 min) with repeated voltage pulses, consistent with previous reports (Roncaglia et al., 2002; Giorgetti et al., 2005).

permit indirect modulation of the VIC by cAMP-responsive factors in addition to the direct effect (or lack thereof) of cAMP binding to the channels.)

VIC Goes through the Normal Pore

Since ZD7288 is thought to be a pore blocker, its block of both I_h and VIC suggests that both currents flow through the central pore of the channel. To confirm this, we used a mutant spHCN channel, spHCN-464C, in which I_h can be blocked irreversibly by binding of Cd^{2+} to cysteines introduced into the pore (Rothberg et al., 2002). From this result, and by analogy with K_v channels (Liu et al., 1997; Long et al., 2005), position 464 in the S6 of spHCN is thought to line the conduction pathway, along the central axis of the protein.

Fig. 3 A shows that Cd^{2+} rapidly blocked VIC when it was applied to spHCN-464C channels at +60 mV. In spHCN-464C, this block was irreversible (as is the block of I_h by Cd^{2+} in spHCN-464C). We also examined the analogous residue in the HCN2 isoform by constructing HCN2-436C, in which a cysteine was introduced into HCN2 at the position corresponding to 464 in spHCN. Application of Cd^{2+} to the intracellular face of HCN2-436C at +60 mV blocked VIC (Fig. 3 E), though in contrast to spHCN-464C, the block of HCN2-436C was rapidly reversible. These effects were specific to the in-

troduced cysteines in the expressed channels, as no block was observed when Cd^{2+} was applied to patches expressing wild-type spHCN or HCN2 channels (Fig. 3, B, D, and F). Together with the block of VIC by ZD7288, these results strongly suggest that VIC and I_h both flow through the main conduction pathway in HCN channels and not through some alternative route (compare Tombola et al., 2005).

VIC Is Produced by a Population of spHCN Channels that Is Not in Rapid Equilibrium with the Voltage-dependent Channel Population

We were surprised to note that the block of VIC by Cd^{2+} in spHCN-464C was qualitatively rather fast (Fig. 3 A). We have previously shown that the Cd^{2+} on-rate for I_h in spHCN-464C varies in parallel with conductance, in a way that is consistent with blocker entry only into open channels (Rothberg et al., 2002). Thus, we expected that the rate of block of VIC should be proportional to the fractional current, or, for spHCN in the presence of cAMP, ~8% of the maximum rate of block (Fig. 2).

(The earlier report (Rothberg et al., 2002) described an ~1,500-fold difference in Cd^{2+} entry rate into spHCN-464C channels at positive versus negative voltages. These experiments reported the rate of block of the total HCN current (the sum of I_h and VIC) because
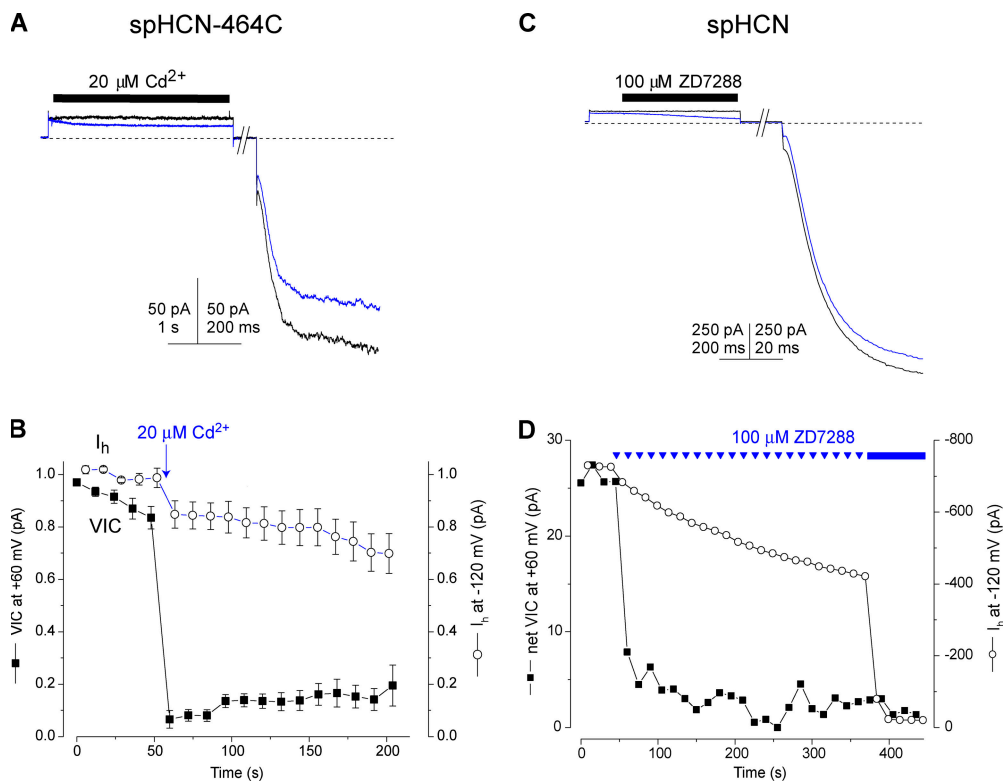
Figure 4. VIC can be blocked independently of I_h. (A) Current traces recorded from a patch expressing spHCN-464C in response to repeated voltage steps to +60 mV and −120 mV. The black trace is the current in the presence of 100 μM cAMP, the blue trace shows the rapid reduction in VIC as 20 μM Cd^{2+} was applied for 5 s, as indicated by the black bar. (B) Average time course of block of VIC and I_h in spHCN-464C after a single 1-s application of 20 μM Cd^{2+} at +60 mV (arrow) in the protocol illustrated in A, with voltage steps given every 12 s. The zero baseline for VIC was taken as the minimum current after Cd^{2+} application. Currents were normalized to the maximum current before Cd^{2+} application. Little recovery of VIC occurred during ∼2 min of repeated pulsing and washing. (C) In the constant presence of 100 μM cAMP, 100 μM ZD7288 was applied to a patch containing spHCN channels during a voltage pulse to +60 mV. Shown are a trace before the application of ZD7288 (black line) and the first trace where ZD7288 was applied (blue line). After a holding period of 8 s at +10 mV, during which all the ZD7288 was washed from the bath, the channels were then stepped to −120 mV to assay the blockade of I_h (note that the block of VIC is also apparent from the initial current at −120 mV, after ZD7288 has been removed). (D) Time course of block of VIC and I_h in response to repeated applications of 100 μM ZD7288 at +60 mV using the protocol illustrated in C, repeated every 15 s. The plotted symbols for VIC represent the current at the start of each pulse to +60 mV, before application of ZD7288; this isolates the irreversible component of block. Complete blockade was elicited after ∼5 min by changing to constant application of ZD7288 (solid bar). Note that no further block of VIC occurred. Net VIC was calculated by subtracting the lowest current measured after blocker application.

the block was assayed by measuring the decrement in steady-state current at negative voltages that resulted from application of Cd^{2+} during prepulses to different potentials. Because the majority of the total current is I_h, the overall rate of Cd^{2+} blockade is highly voltage and state dependent.)

We determined Cd^{2+} entry rates for spHCN-464C at positive and negative voltages by fitting the time course of block at +60 or −120 mV with a single exponential function (Fig. 3, A and C). The resulting decay time constants were used to calculate second-order rate constants. We found that that the rate of block at +60 mV was ∼27% of the rate at −120 mV ($0.96 \pm 0.23 \times 10^5$ $M^{-1}s^{-1}$ at +60 mV, $n = 7$, versus $3.6 \pm 0.4 \times 10^5$ $M^{-1}s^{-1}$ at −120 mV, $n = 4$), considerably faster than would be predicted if VIC were produced by a generally low open probability of HCN channels (if each channel spends ∼8% of its time open at positive voltages, the entry rate should be only ∼8% of that for a channel opened with high probability). Some of this discrepancy could be due to an intrinsic voltage dependence for Cd^{2+} entry (faster at positive voltage), but previous measurements

had shown little or no intrinsic voltage dependence (Fig. 3 of Rothberg et al., 2002).

The anomalously fast block of VIC led us to further experiments, which revealed some unexpected behavior of the voltage-independent current: it behaves as though it is carried by a population of channels that is separate from those that conduct I_h. Patches expressing spHCN-464C channels were repeatedly stepped to +60 mV and then to −120 mV, and the amplitudes of VIC and I_h were monitored. Cd^{2+} was applied only once, during a voltage step to +60 mV (Fig. 4, A and B). This single exposure blocked nearly all of the VIC but only a fraction of I_h. Furthermore, there was little recovery of VIC during several minutes of washing and repeated pulsing (Fig. 4 B; the average recovery at 60 s was $15 \pm 4\%$, $n = 8$). These results would not be expected if the spHCN-464C channels were a single population of channels that simply had a nonzero open probability at positive voltages (schematically shown in Fig. 5 A). In the simplest case, with a rapid equilibrium between open and closed channels at positive voltages, complete block of VIC would occur only when all of the channels
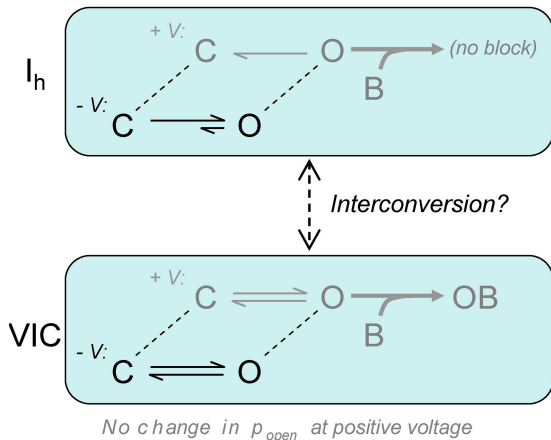
A One Population

Non zero p $_{open}$ at positive voltage permits block
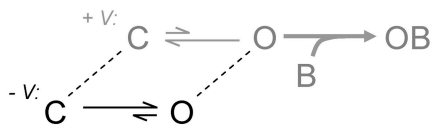
B Two Populations

Figure 5. Two models for the mechanistic basis of VIC, and their response to blocker application at positive voltages. (A) A single population of HCN channels simply fails to close completely at positive voltages. The open channels will be blocked at a rate proportional to p_{open}, and I_h and VIC will be reduced in parallel. (B) Two distinct populations of HCN channels carry I_h and VIC. The I_h channels close completely and are immune to block at positive voltages. The VIC channels have constant (voltage-independent) p_{open} and are blocked at positive voltages.

(voltage dependent as well as voltage independent) had been blocked. If the opening and closing of channels were slow at positive voltages, then the VIC-conducting channels should be completely blocked during the Cd^{2+} application (as we observed), but then subsequent voltage pulses should reestablish the equilibrium among the ~80% of the channels that remain unblocked, and VIC should recover to ~80% of its original amplitude. The actual result, where little recovery occurred in ~2 min, suggests that on this time scale, the channels that conduct VIC are essentially a distinct population of spHCN- 464C channels (as illustrated in Fig. 5 B).

We observed similar behavior using ZD7288 to block wild-type spHCN channels. We applied ZD7288 to spHCN channels, in this case by repeated brief applications at +60 mV, and monitored the effect on both VIC and I_h. We found that VIC was essentially eliminated by the very first application of blocker, whereas I_h was reduced only slowly, as shown by the large difference in the time course of block for VIC and I_h (Fig. 4, C and D).

This parallels the result seen with Cd^{2+} on spHCN-464C and defies the expectation that I_h and VIC would decrease in parallel as ZD7288 (which blocks I_h mostly [~75%] irreversibly; Shin et al., 2001) eliminated the available HCN channels. Again, clearly there is not rapid interconversion between the channels that produce I_h and those that produce VIC.

DISCUSSION

We have examined the VIC produced by HCN channels. We find that VIC flows through expressed HCN channels, and not through an up-regulated endogenous conductance, as it can be blocked by the HCN- specific blocker ZD7288. VIC can also be blocked by Cd^{2+} if (and only if) the expressed HCN channels have cysteine residues introduced at specific sites in the pore.

The simplest explanation for these observations would have been that HCN channels have an appreciable open probability even in the absence of a voltage stimulus or ligand, so that each of the HCN channels in the patch is open a small fraction of the time. Precedent for this idea exists in the unliganded opening of cyclic nucleotide-gated CNG channels (Sunderman and Zagotta, 1999), large conductance mSloI Ca^{2+}-activated (BK) channels (Horrigan et al., 1999), and acetylcholine receptors (Jackson, 1986). This, however, was not the case. Rather, we found, at least for spHCN channels, that VIC is produced by a subset of HCN channels that is not in rapid equilibrium with the main population of voltage-dependent channels. This observation relied on irreversible block of spHCN channels by ZD7288 and by Cd^{2+} (for spHCN-464C); similar experiments were not possible for HCN2 channels because the block by either ZD7288 or Cd^{2+} (in HCN2-436C) was rapidly reversible.

In VIC-producing channels, it is clear that the molecular coupling between the voltage sensors and the gate has failed. This is reminiscent of our description of an unusual mode of inactivation in HCN channels, which appears to result from a slippage in the coupling between the voltage sensors and the gate, so that the main activation gate can close even while the voltage sensors are still activated (Shin et al., 2004). This observation suggests that the coupling between the voltage sensors and the gate in HCN channels is generally weak, and VIC may represent another manifestation of this weak coupling. We showed previously that the seemingly different actions of cAMP on spHCN and the mammalian HCN channels (relief of inactivation in spHCN versus a shift in voltage dependence for mammalian HCNs) can both be explained if the primary effect of cAMP binding is to bias the closed–open equilibrium toward the open state, rather than to increase the strength of coupling between the voltage sensors and the gate (Shin et al., 2004).

The cAMP-dependent increase in VIC we report here is consistent with this mechanism; cAMP acting on the closed–open equilibrium should increase VIC, as we observed, while an increase in coupling strength would have reduced VIC.

What is the mechanism that permits some, but not all, of the HCN channels in a patch to be insensitive to voltage? Are VIC and I_h channels fundamentally different from each other, resulting from a relatively static mechanism such as differential glycosylation or differential association with accessory subunits? Or is the difference between VIC and I_h channels the result of a more transient modification such as phosphorylation, which may permit rapid interconversion under some circumstances?

Precedents exist for both of these scenarios. On one hand, voltage-dependent KCNQ1 (KvLQT1) channels can coassemble with some members of the MiRP (KCNE) family of single transmembrane-spanning proteins to produce a voltage-independent K^+ current (Schroeder et al., 2000; Tinel et al., 2000). HCN channels can also associate with MiRPs (Yu et al., 2001; Decher et al., 2003; Qu et al., 2004), and coexpression of MiRP1 (KCNE2) with HCN2 increases the voltage-independent current and decreases the voltage-dependent current (Proenza et al., 2002).

In AKT2 and KCNK2 channels, on the other hand, PKA-mediated phosphorylation determines whether the channels are voltage dependent or voltage independent (Bockenhauer et al., 2001; Dreyer et al., 2001; Michard et al., 2005a,b). In single channel records, voltage-independent gating appears as a distinct mode, and rapid transitions between gating modes can be observed in single patches, clearly indicating that AKT2 and KCNK2 channels are not divided into separate populations. Interestingly, the phosphorylation sites that govern the gating transition in AKT2 are in the S4–S5 linker and lower S6 transmembrane domain, regions that have been implicated in coupling between the voltage sensors and the gates in HCN and other channels (Chen et al., 2001; Lu et al., 2002; Ding and Horn, 2003; Decher et al., 2004).

Our observation of two populations of HCN channels appears to be more consistent with a relatively static mechanism of voltage-independent gating. However, since our experiments were conducted in excised inside-out patches, which lack most potential regulatory elements, it is not clear whether two separate populations of HCN channels would be present in intact cells. The slow interconversion we observed between VIC and I_h hints that modulatory elements may also regulate voltage-independent gating in HCN channels.

Physiological Significance of VIC

In contrast to K^+ leak currents, which tend to dampen excitability by clamping the membrane voltage near the K^+ reversal potential, the voltage-independent current produced by HCN channels would tend to promote excitability because it is a mixed cationic conductance with a reversal potential of ~ -20 mV. Thus in neurons or cardiomyocytes, inward VIC current flowing at hyperpolarized potentials would tend to depolarize the cells toward the action potential threshold, and outward current flowing through open VIC channels at depolarized potentials would tend to speed repolarization from the peak of an action potential. In the sinoatrial node of the heart, HCN channels are critical for the development of the mature diastolic depolarization and for its response to sympathetic stimulation (Stieber et al., 2003). However, the precise mechanism for the channels' involvement is unclear because the threshold for activation is rather negative compared with the maximum diastolic potential. This can be seen in recent studies of isolated mouse sinoatrial myocytes, in which the maximum diastolic potential is ~ -60 mV, a potential at which there is very little activation of I_f (Mangoni and Nargeot, 2001; Cho et al., 2003). If native HCN channels produce VIC of a magnitude similar to that described here for heterologously expressed HCN channels, the voltage-independent current is likely to contribute significantly to the pacemaker depolarization.

REFERENCES

Bockenhauer, D., N. Zilberberg, and S.A. Goldstein. 2001. KCNK2: reversible conversion of a hippocampal potassium leak into a voltage-dependent channel. *Nat. Neurosci.* 4:486–491.

Brown, H., and D. DiFrancesco. 1980. Voltage-clamp investigations of membrane currents underlying pace-maker activity in rabbit sino-atrial node. *J. Physiol.* 308:331–351.

Brown, H.F., D. DiFrancesco, and S.J. Noble. 1979. How does adrenaline accelerate the heart? *Nature.* 280:235–236.

Cho, H.S., M. Takano, and A. Noma. 2003. The electrophysiological properties of spontaneously beating pacemaker cells isolated from mouse sinoatrial node. *J. Physiol.* 550:169–180.

Chen, J., J.S. Mitcheson, M. Tristani-Firouzi, M. Lin, and M.C. Sanguinetti. 2001. The S4-S5 linker couples voltage sensing and activation of pacemaker channels. *Proc. Natl. Acad. Sci. USA.* 98:11277–11282.

Decher, N., F. Bundis, R. Vajna, and K. Steinmeyer. 2003. KCNE2 modulates current amplitudes and activation kinetics of HCN4: influence of KCNE family members on HCN4 currents. *Pflugers Arch.* 446:633–640.

Decher, N., J. Chen, and M.C. Sanguinetti. 2004. Voltage-dependent gating of hyperpolarization-activated, cyclic nucleotide-gated pacemaker channels: molecular coupling between the S4-S5 and C-linkers. *J. Biol. Chem.* 279:13859–13865.

Ding, S., and R. Horn. 2003. Effect of S6 tail mutations on charge movement in Shaker potassium channels. *Biophys. J.* 84:295–305.

Dreyer, I., E. Michard, B. Lacombe, and J.B. Thibaud. 2001. A plant Shaker-like K$^+$ channel switches between two distinct gating modes resulting in either inward-rectifying or "leak" current. *FEBS Lett.* 505:233–239.

Gauss, R., R. Seifert, and U.B. Kaupp. 1998. Molecular identification of a hyperpolarization-activated channel in sea urchin sperm. *Nature.* 393:583–587.

Giorgetti, A., P. Carloni, P. Mistrik, and V. Torre. 2005. A homology model of the pore region of HCN channels. *Biophys. J.* 89:932–944.

Halliwell, J.V., and P.R. Adams. 1982. Voltage-clamp analysis of muscarinic excitation in hippocampal neurons. *Brain Res.* 250:71–92.

Hamill, O.P., A. Marty, E. Neher, B. Sakmann, and F.J. Sigworth. 1981. Improved patch-clamp techniques for high-resolution current recording from cells and cell-free membrane patches. *Pflugers Arch.* 391:85–100.

Horrigan, F.T., J. Cui, and R.W. Aldrich. 1999. Allosteric voltage gating of potassium channels I. mSlo ionic currents in the absence of Ca^{2+}. *J. Gen. Physiol.* 114:277–304.

Ishii, T.M., M. Takano, L.H. Xie, A. Noma, and H. Ohmori. 1999. Molecular characterization of the hyperpolarization-activated cation channel in rabbit heart sinoatrial node. *J. Biol. Chem.* 274:12835–12839.

Jackson, M.B. 1986. Toward a mechanism of gating of chemically activated channels. *Adv. Neurol.* 44:171–189.

Jurman, M.E., L.M. Boland, Y. Liu, and G. Yellen. 1994. Visual identification of individual transfected cells for electrophysiology using antibody-coated beads. *Biotechniques.* 17:876–881.

Liu, Y., M. Holmgren, M.E. Jurman, and G. Yellen. 1997. Gated access to the pore of a voltage-dependent K$^+$ channel. *Neuron.* 19:175–184.

Long, S.B., E.B. Campbell, and R. MacKinnon. 2005. Crystal structure of a mammalian voltage-dependent Shaker family K$^+$ channel. *Science.* 309:897–903.

Lu, Z., A.M. Klem, and Y. Ramu. 2002. Coupling between voltage sensors and activation gate in voltage-gated K$^+$ channels. *J. Gen. Physiol.* 120:663–676.

Ludwig, A., X. Zong, M. Jeglitsch, F. Hofmann, and M. Biel. 1998. A family of hyperpolarization-activated mammalian cation channels. *Nature.* 393:587–591.

Macri, V., and E.A. Accili. 2004. Structural elements of instantaneous and slow gating in hyperpolarization-activated cyclic nucleotide-gated channels. *J. Biol. Chem.* 279:16832–16846.

Mangoni, M.E., and J. Nargeot. 2001. Properties of the hyperpolarization-activated current (I$_f$) in isolated mouse sino-atrial cells. *Cardiovasc. Res.* 52:51–64.

Michard, E., I. Dreyer, B. Lacombe, H. Sentenac, and J.B. Thibaud. 2005a. Inward rectification of the AKT2 channel abolished by voltage-dependent phosphorylation. *Plant J.* 44:783–797.

Michard, E., B. Lacombe, F. Poree, B. Mueller-Roeber, H. Sentenac, J.B. Thibaud, and I. Dreyer. 2005b. A unique voltage sensor sensitizes the potassium channel AKT2 to phosphoregulation. *J. Gen. Physiol.* 126:605–617.

Pape, H.C., and D.A. McCormick. 1989. Noradrenaline and serotonin selectively modulate thalamic burst firing by enhancing a hyperpolarization-activated cation current. *Nature.* 340:715–718.

Proenza, C., D. Angoli, E. Agranovich, V. Macri, and E.A. Accili. 2002. Pacemaker channels produce an instantaneous current. *J. Biol. Chem.* 277:5101–5109.

Qu, J., Y. Kryukova, I.A. Potapova, S.V. Doronin, M. Larsen, G. Krishnamurthy, I.S. Cohen, and R.B. Robinson. 2004. MiRP1 modulates HCN2 channel expression and gating in cardiac myocytes. *J. Biol. Chem.* 279:43497–43502.

Roncaglia, P., P. Mistrik, and V. Torre. 2002. Pore topology of the hyperpolarization-activated cyclic nucleotide-gated channel from sea urchin sperm. *Biophys. J.* 83:1953–1964.

Rothberg, B.S., K.S. Shin, P.S. Phale, and G. Yellen. 2002. Voltage-controlled gating at the intracellular entrance to a hyperpolarization-activated cation channel. *J. Gen. Physiol.* 119:83–91.

Rothberg, B.S., K.S. Shin, and G. Yellen. 2003. Movements near the gate of a hyperpolarization-activated cation channel. *J. Gen. Physiol.* 122:501–510.

Santoro, B., S.G. Grant, D. Bartsch, and E.R. Kandel. 1997. Interactive cloning with the SH3 domain of N-src identifies a new brain specific ion channel protein, with homology to eag and cyclic nucleotide-gated channels. *Proc. Natl. Acad. Sci. USA.* 94:14815–14820.

Santoro, B., D.T. Liu, H. Yao, D. Bartsch, E.R. Kandel, S.A. Siegelbaum, and G.R. Tibbs. 1998. Identification of a gene encoding a hyperpolarization-activated pacemaker channel of brain. *Cell.* 93:717–729.

Schroeder, B.C., S. Waldegger, S. Fehr, M. Bleich, R. Warth, R. Greger, and T.J. Jentsch. 2000. A constitutively open potassium channel formed by KCNQ1 and KCNE3. *Nature.* 403:196–199.

Seed, B., and A. Aruffo. 1987. Molecular cloning of the CD2 antigen, the T-cell erythrocyte receptor, by a rapid immunoselection procedure. *Proc. Natl. Acad. Sci. USA.* 84:3365–3369.

Shin, K.S., C. Maertens, C. Proenza, B.S. Rothberg, and G. Yellen. 2004. Inactivation in HCN channels results from reclosure of the activation gate: desensitization to voltage. *Neuron.* 41:737–744.

Shin, K.S., B.S. Rothberg, and G. Yellen. 2001. Blocker state dependence and trapping in hyperpolarization-activated cation channels: evidence for an intracellular activation gate. *J. Gen. Physiol.* 117:91–101.

Stieber, J., S. Herrmann, S. Feil, J. Loster, R. Feil, M. Biel, F. Hofmann, and A. Ludwig. 2003. The hyperpolarization-activated channel HCN4 is required for the generation of pacemaker action potentials in the embryonic heart. *Proc. Natl. Acad. Sci. USA.* 100:15235–15240.

Sunderman, E.R., and W.N. Zagotta. 1999. Mechanism of allosteric modulation of rod cyclic nucleotide-gated channels. *J. Gen. Physiol.* 113:601–620.

Tinel, N., S. Diochot, M. Borsotto, M. Lazdunski, and J. Barhanin. 2000. KCNE2 confers background current characteristics to the cardiac KCNQ1 potassium channel. *EMBO J.* 19:6326–6330.

Tombola, F., M.M. Pathak, and E.Y. Isacoff. 2005. Voltage-sensing arginines in a potassium channel permeate and occlude cation-selective pores. *Neuron.* 45:379–388.

Yu, H., J. Wu, I. Potapova, R.T. Wymore, B. Holmes, J. Zuckerman, Z. Pan, H. Wang, W. Shi, R.B. Robinson, et al. 2001. MinK-related peptide 1: A β subunit for the HCN ion channel subunit family enhances expression and speeds activation. *Circ. Res.* 88:E84–E87.